

PROCEEDINGS OF SPIE

[SPIDigitalLibrary.org/conference-proceedings-of-spie](https://spiedigitallibrary.org/conference-proceedings-of-spie)

Design, testing, and performance of the Hobby Eberly Telescope prime focus instrument package

Vattiat, Brian, Hill, Gary, Lee, Hanshin, Perry, Dave, Rafal, Marc, et al.

Brian Vattiat, Gary J. Hill, Hanshin Lee, Dave M. Perry, Marc D. Rafal, Tom Rafferty, Richard Savage, Charles A. Taylor III, Walter Moreira, Michael Smith, "Design, testing, and performance of the Hobby Eberly Telescope prime focus instrument package," Proc. SPIE 8446, Ground-based and Airborne Instrumentation for Astronomy IV, 844672 (24 September 2012); doi: 10.1117/12.926413

SPIE.

Event: SPIE Astronomical Telescopes + Instrumentation, 2012, Amsterdam, Netherlands

Design, testing, and performance of the Hobby Eberly Telescope prime focus instrument package

Brian Vattiat^a, Gary J. Hill^a, Hanshin Lee^a, Dave M Perry^a, Marc D Rafal^a, Tom Rafferty^a, Richard Savage^a, Charles A Taylor III^a, Walter Moreira^a, Michael Smith^b

^aMcDonald Observatory, Univ. of Texas at Austin, 1 University Station C1402, Austin, TX 78712, USA; ^bDepartment of Astronomy, 2535 Sterling Hall, 475 N. Charter Street, Madison, WI 53706, USA

ABSTRACT

The Hobby-Eberly Telescope (HET) is undergoing an upgrade to increase the field of view to 22 arc-minutes with the dark energy survey HETDEX the initial science goal [1]. Here we report on the engineering development of a suite of instruments located at prime focus of the upgraded HET. The Prime Focus Instrument Package (PFIP) contains acquisition, guiding, and wave front sensing instrumentation [2], the fiber feeds for the facility spectrographs (VIRUS, HRS, MRS, LRS2), and ancillary hardware. This paper reviews the design and functions of the PFIP and presents details of the mechanical design, integration and testing.

Keywords: HETDEX, HET, Hobby Eberly Telescope, VIRUS

1. INTRODUCTION

The Hobby Eberly Telescope (HET) is a unique telescope built in far west Texas. The telescope primary mirror consists of 91 individual spherical segments mounted on a structure with fixed altitude and moveable azimuth. The Prime Focus Instrument Package is mounted to a 6 degree-of-freedom stage [3],[4] above the primary mirror, allowing the telescopes field of view to track celestial objects.

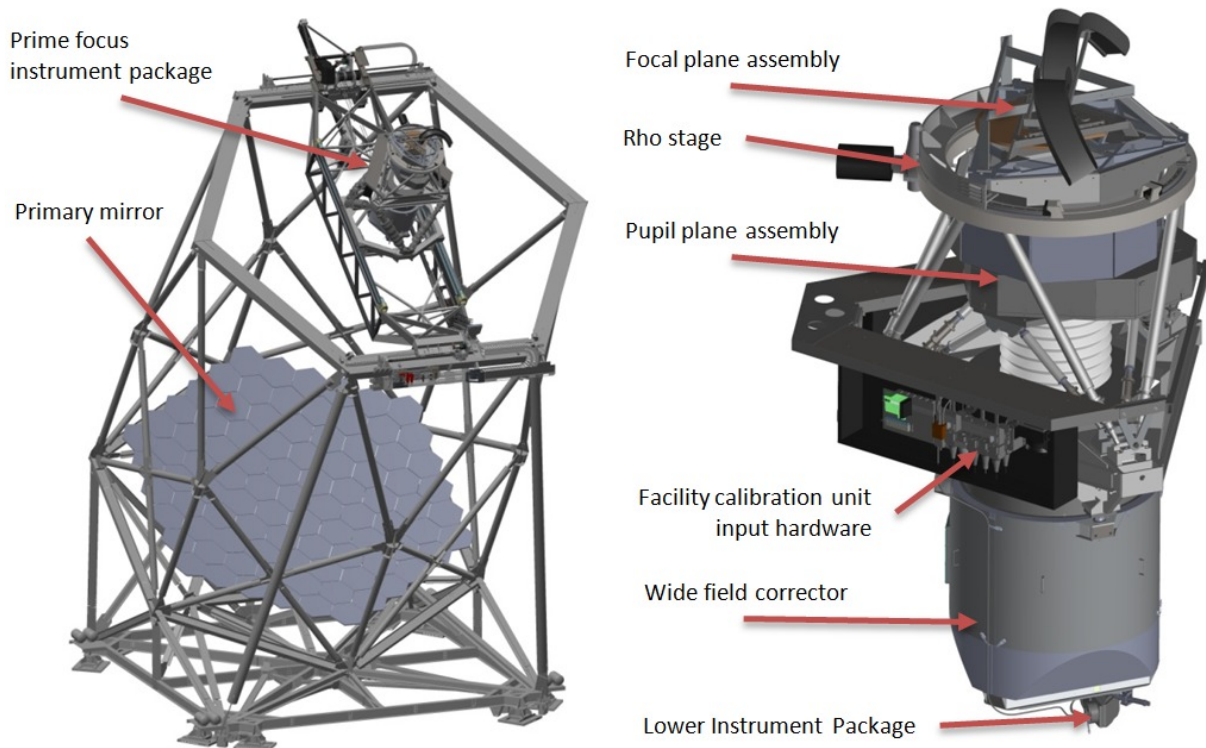


Figure 1. Renderings of the HET telescope and the prime focus instrument package

The PFIP consists of several subassemblies. The Wide Field Corrector (WFC) focuses a corrected image from light gathered by the primary mirror and is covered in detail elsewhere [5]. The focal plane assembly (FPA), shown in figure 2, contains all the hardware at the focus of the telescope including the acquisition and guiding (AG) assembly, fiber instrument feeds, shutter, and electronics hardware. The FPA is mounted to the Rho stage, allowing the FPA to be rotated along the optical axis and track parallactic angle. The Lower Instrument Package (LIP) is mounted to the input end of the wide field corrector and is a platform for the entrance window changer, tip-tilt camera, and facility calibration unit (FCU) output head. A set of temperature controlled, insulated enclosures house electronics hardware and the facility calibration unit input hardware. The pupil plane assembly (PPA) is located in between the wide field corrector and the focal plane assembly. It contains a stationary and moving set of baffles and a platform for exit windows for the wide field corrector and an atmospheric dispersion corrector.

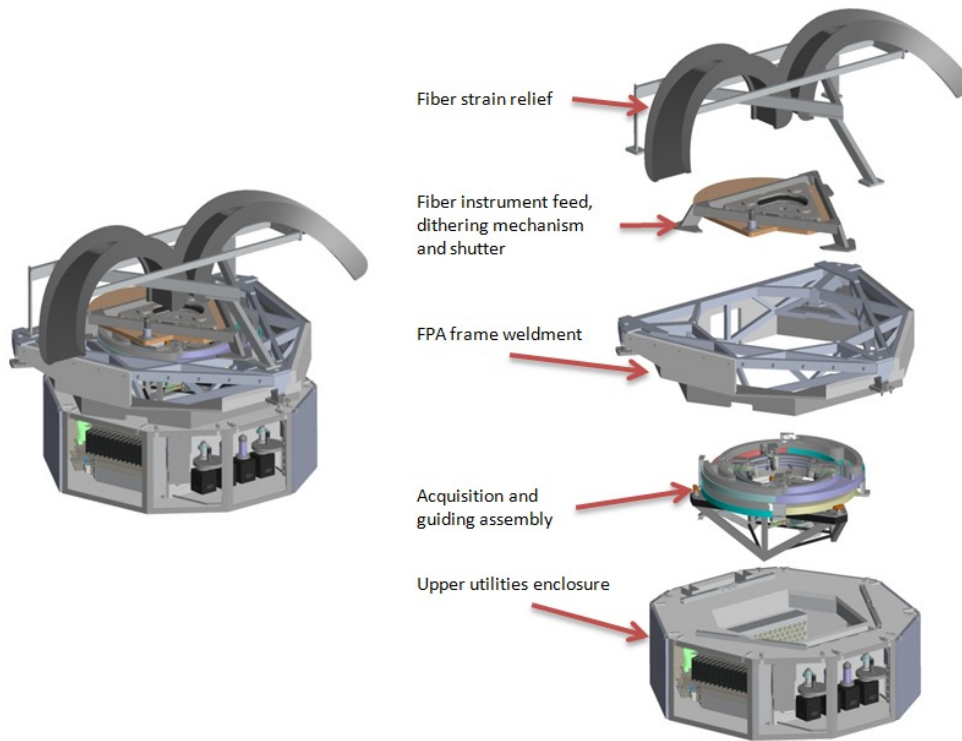


Figure 2. Rendering of the focal plane assembly and its subassemblies

2. DESIGN

2.1 Guide Probe Assembly

The guide probe assembly is used for star guiding of the telescope. There are four probes; two imaging probes and two wave-front sensing probes. Each probe consists of a probe optical head, containing the necessary optics coupled to a coherent fiber bundle purchased from Schott. Images incident to the fiber bundle input are captured by a remote camera system at the bundle output. Each probe optical head is mounted to an arm for moving the probe radially in the field with a range of 8-11 arcminutes from the center of the telescope's field. Each arm is mounted to a carriage which can travel 180 degrees around the perimeter of the field. The arm axis is at angle to the carriage axis such that motion of the probe head follows a sphere for all angles. Figure 3 illustrates the guide probe assembly. Figure 4 illustrates the arm axis (φ) and the carriage axis (θ).

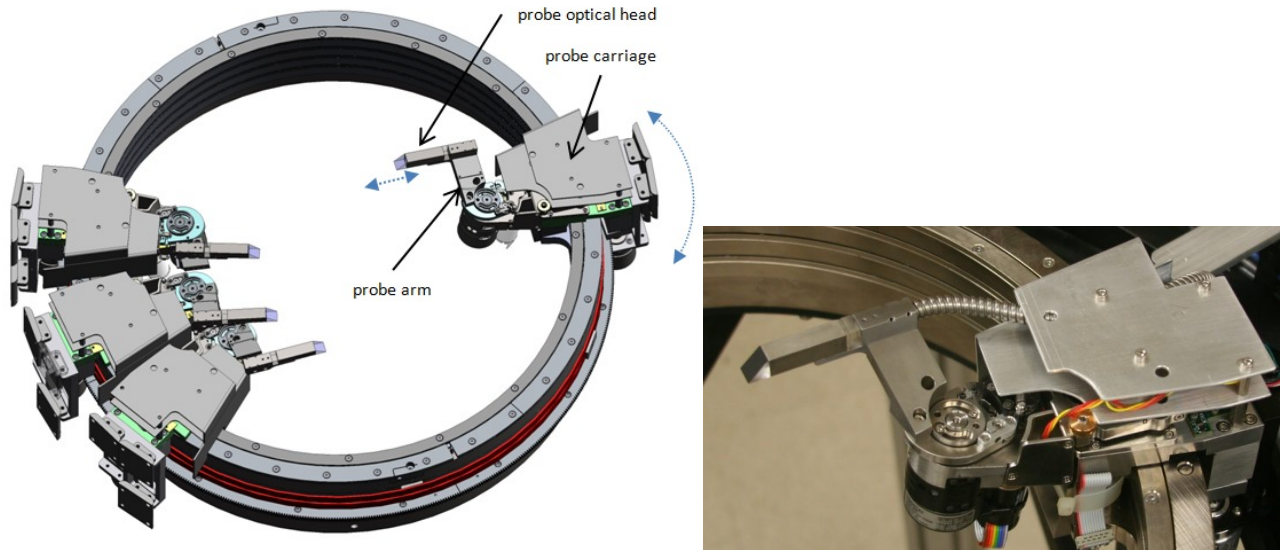


Figure3. Illustration and photo of guider probe assembly mechanics

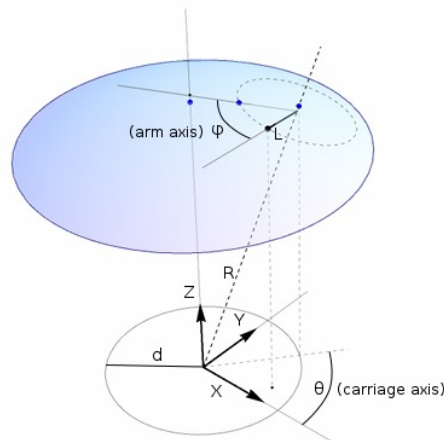


Figure 4. Illustration of guider θ (carriage axis) and ϕ (arm axis) on a spherical surface.

The positioning accuracy requirement of the guide probes is 20 microns on the spherical focal surface. To achieve this, both mechanical position actuation and encoding required a high level of precision. For the arm axis, mechanical position is actuated by a Maxon EC max 22 motor and gear head turning a wire rope capstan. The wire rope capstan provides a means to offset the motor and gearbox axis from the arm axis with a compliant and cogless transmission. Any backlash in the system is biased with an extension spring. A set of adjustable pre-loaded angular contact bearings support the arm axis. The arm axis encoder is a Hengstler AD34 magnetic rotary encoder with 17 bits of single-turn resolution. The encoder axis is rigidly coupled to the arm axis and the encoder body is mounted to the carriage chassis through a flexural bracket. For the carriage axis, an identical Maxon motor and gearbox is coupled to a toothed-belt pulley idler driving a wire-rope capstan. Each carriage is mounted to one in a stack of Kaydon bearings, furnished with a factory-set preload. The carriage axis encoder is a Lika linear magnetic encoder reading a flexible tape wrapped on the outer diameter of the carriage bearing stack. The encoder has 5 micron resolution with index marks at 2mm but is incremental, not absolute. To achieve “power-on” absolute encoding a second encoder is used. A Hengstler magnetic rotary encoder AC36 is coupled to a pinion gear which meshes to a rack of gear teeth on the outer perimeter of the carriage bearing stack. This encoding solution has absolute position measurement but suffers from backlash and cogging due to the geared interface. It therefore cannot be used for position control but instead is used to reference the coarsely

spaced index marks of the Lika incremental encoder. Upon “power-on”, the carriage is driven to the nearest index mark of the incremental encoder which is achieved with high repeatability. The absolute encoder position is read and the value is referenced to a look-up-table relating ranges of absolute encoder to incremental encoder index positions.

At this time, the guide probe assembly is operational and undergoing tests and alignment procedures. Computer control of the assembly is accomplished using a National Instruments LabView program and the Maxon-supplied LabView instrument drivers. A simple graphical interface was created to allow position control of the assembly, and preconfigured routines of position changes. One test completed so far is mapping the spherical surface for a probe and measuring run-out from that surface due to bearing imperfections. The test utilized an API Traker3™ laser tracker mounted on a mast above the guide probe assembly tracking a ½ inch ball-mounted retro reflector mounted on a guide probe arm, figure 5. The guide probe is run through a raster pattern routine, with laser tracker measurements taken every 1mm of probe motion. A sphere is fit to the recorded points using New River Kinematics’ Spatial Analyzer® software. Deviations of the measurement data from the fit sphere can be visualized in a vector plot, shown in Figure 6. The maximum deviation was measured to be 31 microns, corresponding to ~0.05 arcseconds defocus.

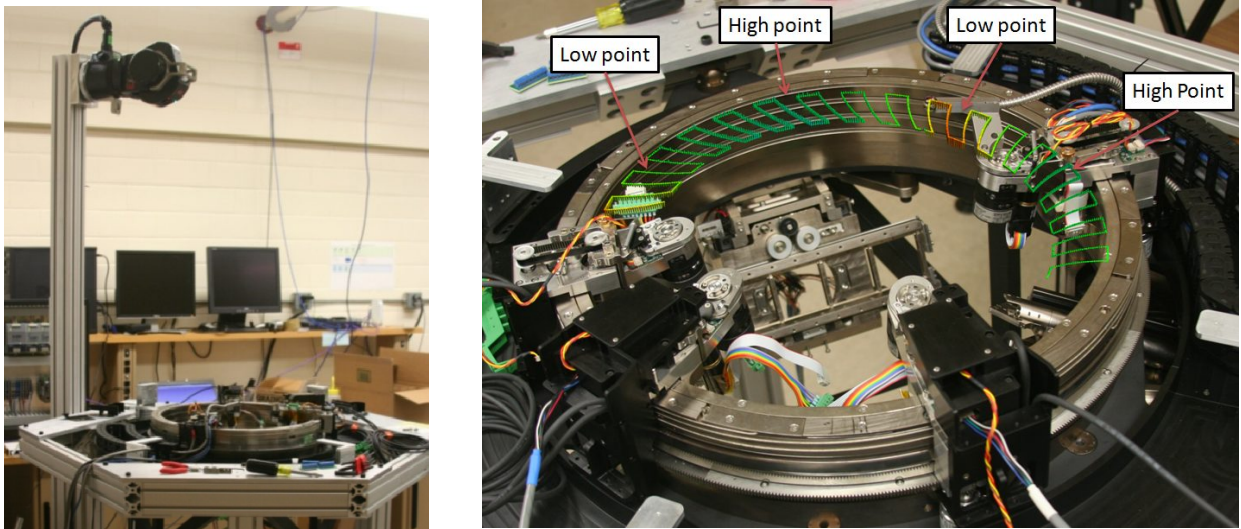


Figure 5, left showing API laser tracker mass mounted above the guide probe assembly. Figure 6, right showing vector plot of guide probe deviations from spherical fit measured along the raster pattern routine.

The next tests will involve measuring the absolute positioning accuracy of the guide probes. A series of tests will compare the x,y,z position of the guide probe calculated from the rotary encoder positions to the x,y,z position measured by the API laser tracker. In order to do this, a set of equations is needed to transform the angles measured from the arm and carriage encoders to x, y, and z positions.

$$x = R \sin(r) \cos(\theta')$$

$$y = R \sin(r) \sin(\theta')$$

$$z = R \cos(r)$$

where

$$r = \arccos\left(\frac{\sqrt{R^2 - L^2} \sqrt{R^2 - d^2} + Ld \cos(\varphi)}{R^2}\right)$$

$$\theta' = \theta - \arctan\left(\frac{RL \sin(\varphi)}{d\sqrt{R^2 - L^2} - L\sqrt{R^2 - d^2} \cos(\varphi)}\right)$$

2.2 Guide Probe Cameras

Each of the guide probes is equipped with a coherent fiber bundle; the input end mounted the guide probe optical head and the output mounted to a guide probe camera. The camera system contains a set of relay optics and FLI Microline ML261E CCD with liquid cooled TEC. The fiber bundle output interface is designed such that the rows and columns of

fibers in the bundle can be rotated to match the rows and columns of pixels in the CCD detector. In the case of the imaging probes, a custom filter wheel is also used. The filter wheel holds 5x50mm diameter filters and is directly driven by the same model Maxon ECmax 20 motor and gear head used with the guide probes. The drive system uses an incremental encoder mounted to the motor shaft for position encoding, however 5 hall effect switches are used to locate individual filters. A magnet is embedded in the filter wheel and the 5 hall switches are mounted to the chassis, with one switch triggered for each filter position. The hall switches are connected to the digital inputs on the Maxon motor controller and a homing mode is used to automatically drive the filter wheel to the desired filter position. Figure 7 shows a model of the imaging probe camera system. For the wave-front measurement probes, no filter wheel is needed and an off-the-shelf relay lens assembly from Edmund Optics was integrated into a custom mechanical housing, shown in figure 8.

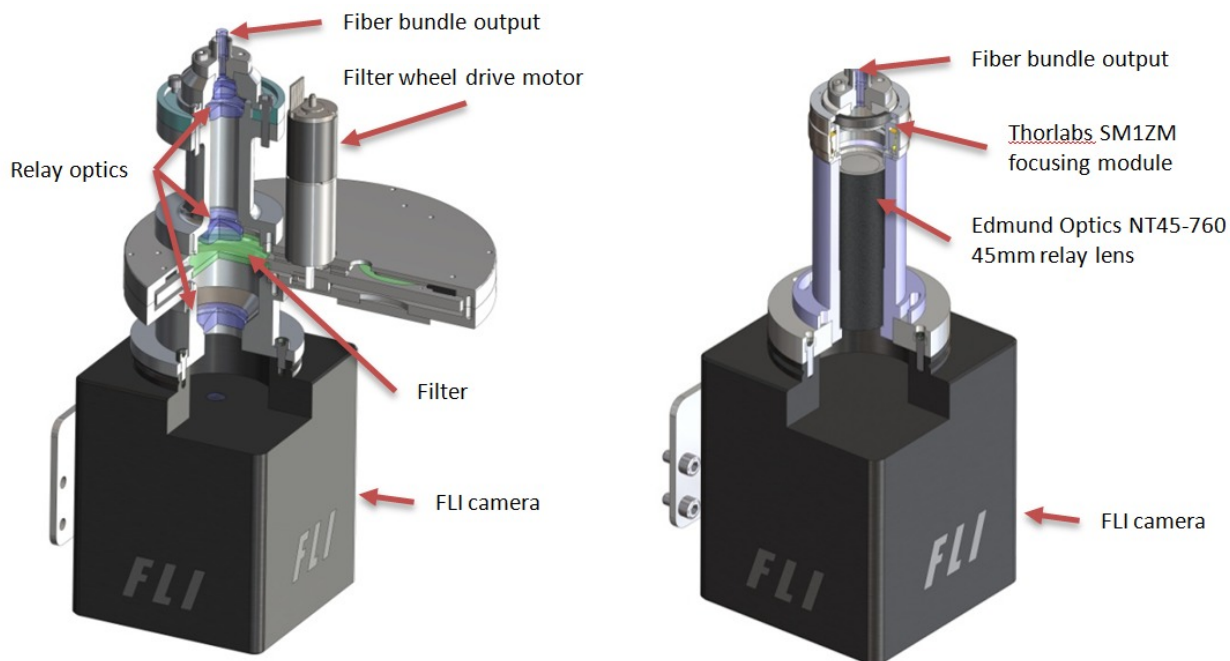


Figure 7, left showing a sectioned model of the imaging probe camera system. Figure 8, right showing a sectioned model of the wave-front measuring probe camera system.

2.3 Shutter

The prime focus shutter is a rotary-type shutter initially inspired by the FORS shutter design; the shutter “blade” is a rotating disc with an aperture cut out of one section. Exposure occurs when the disc rotates so that the aperture aligns with the clear aperture of the focal surface. The shutter blade itself is a custom cut sheet of carbon fiber reinforced plastic (CFRP) purchased from Allred Associates. The shutter blade is fastened to a hardened steel ring. The inner diameter of the ring has a vee profile, which rides on 6 ball-bearing guide wheels mounted to the shutter chassis. The outer diameter of the ring has a toothed profile which meshes with a Kevlar reinforced toothed drive belt. The belt is driven by a toothed pulley mounted to a Maxon EC-max 40 motor and 15:1 reduction planetary gear head. An absolute rotary encoder is mounted at the center of the shutter blade. A flexural mount on the encoder body ensures concentricity between encoder axis and shutter axis. The encoder is a Hengstler AC36 with 13bit single-turn resolution and 12bit multi-turn resolution. The encoder has a SSI interface which reports position directly to the Maxon EPOS2 50/5 positioning controller. Figure 9 illustrates the basic mechanical design.

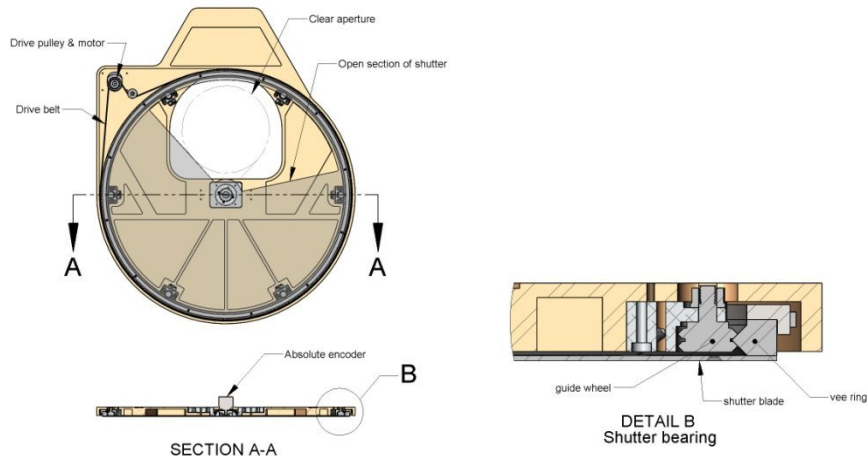


Figure 9. Mechanical design for prime focus shutter drive.

The timing and position control of the shutter is achieved using position, velocity, and time (PVT) trajectory interpolation mode on the EPOS2 controller. When an exposure is executed, the control computer streams a series of PVT points to a buffer in the EPOS2 controller. These control points are spaced with 1-255ms intervals and the controller interpolates between those points using cubic spline interpolation with millisecond resolution. The trajectory is generated by a software algorithm on the control computer. First, a series of waypoints are computed for key locations on the trajectory. Those waypoints are parametric to the exposure duration, shutter geometry, and maximum acceleration. Figure 10 illustrates these waypoints and Table 1 shows formula for computing the time for each waypoint. Once the waypoints are calculated, the trajectory can be computed by applying a kinematic interpolation which assumes constant acceleration between waypoints. The algorithm for interpolation is shown in Table 2. Figure 11 shows a plot of the trajectory with 50ms intervals and the waypoints on which they were based.

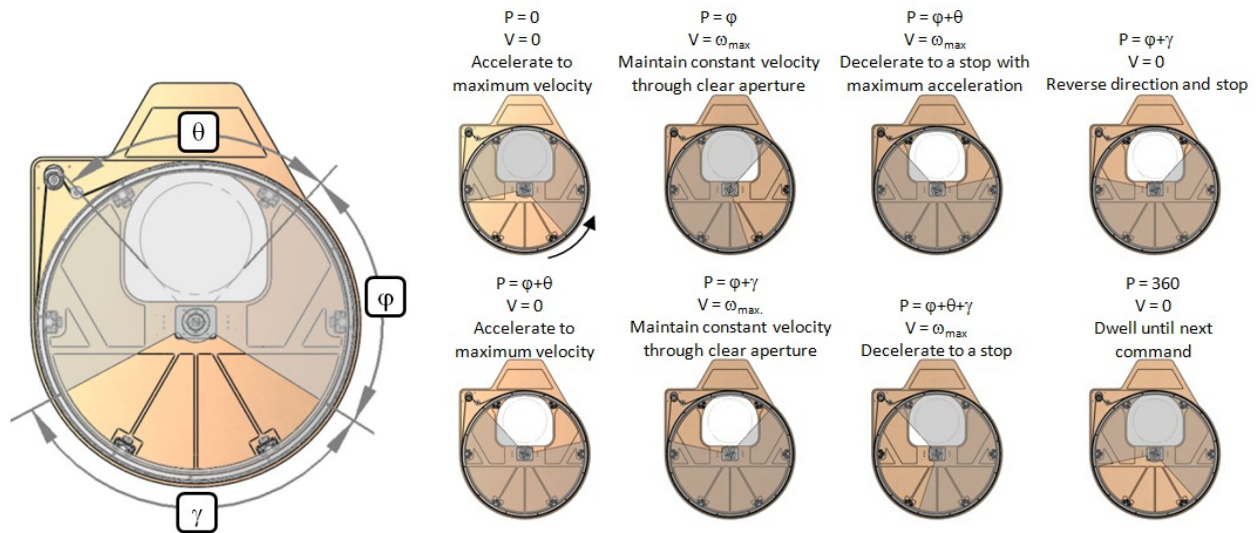


Figure 10. Waypoints for shutter trajectory

$$\omega_{max} = (2 * \omega'_{max}(\theta - \gamma))^{1/2} \quad \Delta_1 = 2 \frac{\varphi}{\omega_{max}} \quad \Delta_2 = \frac{\theta}{\omega_{max}} \quad \Delta_3 = 2 \frac{(\gamma - \theta)}{\omega_{max}} \quad \Delta_4 = \Delta_5 = \left(\frac{\gamma - \theta}{\omega'_{max}} \right)^{1/2}$$

$$\Delta_6 = T_{exposure} - \Delta_2 - \Delta_3 - \Delta_4 - \Delta_5 - \Delta_7 \quad \Delta_7 = 2 \frac{(\gamma - \theta)}{\omega_{max}} \quad \Delta_8 = \frac{\theta}{\omega_{max}} \quad \Delta_9 = \frac{2(360 - \varphi - \gamma - \theta)}{\omega_{max}}$$

Table 1. Formula for computing waypoint times.

For a time t which is between waypoints T_n and T_{n+1} , and where the corresponding waypoint velocities are V_n and V_{n+1} and waypoint positions P_n and P_{n+1} :

$$V_t = V_N + \frac{V_{N+1} - V_N}{T_{N+1} - T_N} (t - T_N)$$

$$P_t = P_N + \frac{V_t - V_N}{2} (t - T_N)$$

Table 2. Formula for computing trajectories from waypoints

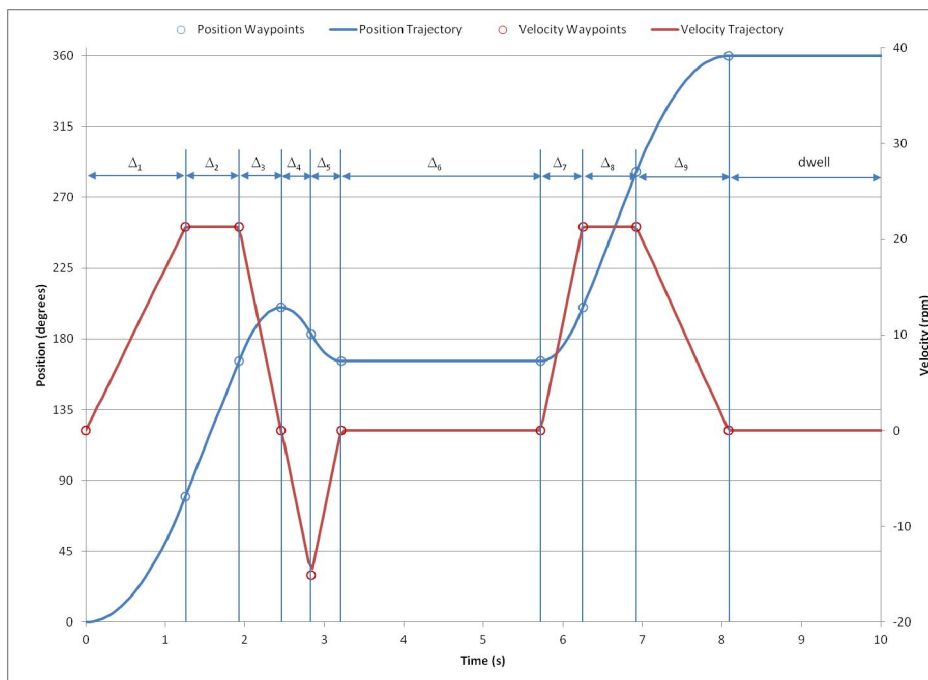


Figure 11. Shutter position and velocity trajectory for a 5s exposure.

2.4 Dithering Mechanism and Fiber Feed Plate

The dithering mechanism is a three position actuator that offsets the fiber feeds so that a set of three exposures will fill the interstitial space between fibers in a single VIRUS IFU. The device is actuated by six Festo “fluidic muscle” DSMP pneumatic actuators; two are active in each of three positions. These actuators were selected for their high initial force and small diameter. They are particularly well suited for short-throw applications. A special pin flexure was designed to control the motion of the dithering mechanism. The design required a ~150 micron movement in a plane normal to the optical axis but only allowed for ~5 micron motion parallel to the optical axis despite the varying loads from the fiber feeds. Initial designs called for a set of nested X and Y blade flexures but those were too compliant axially. The pin flexure takes the properties of a long, slender pin; high axial stiffness and low shear stiffness. By combining many parallel pins, the required axial strength can be achieved while keeping the shear stiffness low enough to be pneumatically actuated. Each flexure consists of 127 pins fabricated by cutting a single piece of 1.25/1.0/25 Grade 5 titanium with a wire electrical discharge machine (EDM) from three orientations (figures 12 and 13). Three flexures are used in the dithering mechanism; one at each corner of the triangular assembly. A set of locating pins and adjustable stops allow the stroke of the mechanism to be fine tuned.

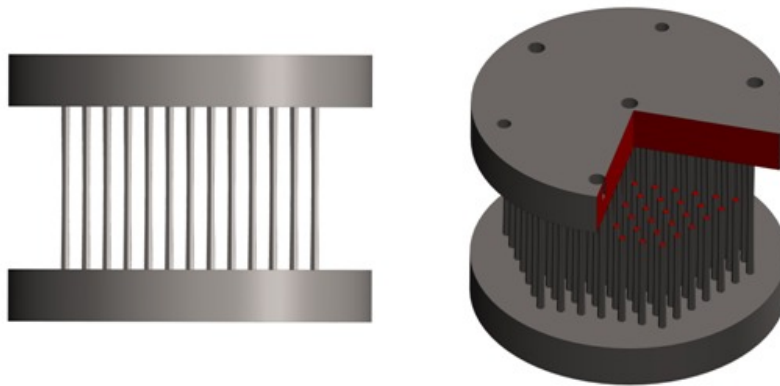


Figure 12, left shows the dithering flexure along one of three identical cutting axes. Figure 13, right shows a sectional view of the flexure.

The fiber feed mounting plate is mounted to the moving portion of the dithering mechanism and serves to provide mounting points for all the fiber feeds. The orientation and location of the fiber feed mounting points require a high level of precision. All mounting points are oriented such that the input tips of the fiber feeds follow the spherical focal surface. The mounting points have tight tolerance bores for precise locating and repeatability of the fiber feeds. The mounting plate has 100 mounting points for VIRUS-style fiber feeds and a central mounting locating for the HET's Medium resolution spectrograph, High resolution spectrograph, and a future instrument. The central mounting location will also be used to mount hardware required for the telescopes alignment. The fiber feed plate will begin fabrication after the WFC is completed and the radius of the best focus surface is determined. Figure 14 shows an exploded CAD view of the dithering mechanism and fiber feed plate. Figure 15 shows a photo of the assembly. Initial testing of the mechanism was performed using a stationary digital camera taking images of a precision optical grid target mounted on the moving portion. The dithering motions were found to be repeatable and an automated test using a laser tracker will be performed in the future.



Figure 14, left shows an exploded rendering of the dithering mechanism and the fiber feed mounting plate. Figure 15, right shows a photo of the dithering mechanism and shutter underneath.

2.5 Acquisition Camera

The acquisition camera (figure 16) is located beneath the guide probe assembly and contains a Finger Lakes Imaging ML090000 with liquid-cooled TEC. It has a 1 arcminute field of view about the center of the telescope field. The camera is fed light by a pneumatically deployed fold mirror. The camera is able to focus +/-15mm from nominal along a pair of adjustable preload THK HR1530 ball guides. Actuation is by a miniature ball screw purchased from Misumi and turned by the same Maxon ECmax 22 motor and gear head used in the guide probe assembly and elsewhere. A Lika SMA5 linear magnetic absolute encoder with 5 micron resolution is used to measure focus position. Its SSI interface is connected directly to the Maxon EPOS2 motor controller for position control.

The acquisition camera includes a four position filter changer for 50mm square filters. The filter magazine rides on a set of adjustable preload ball guides purchased from Misumi. A toothed belt is stretched along an edge of the magazine and through two idlers and a drive pulley. The drive pulley is turned by one of the same Maxon motor and gear heads. Four hall effect switches are mounted to the chassis and triggered by two magnets on the filter magazine. Each hall effect switch corresponds to a filter position and their outputs are wired to the Maxon motor controller. A homing mode is used to drive the magazine position until the desired hall effect switch is triggered.

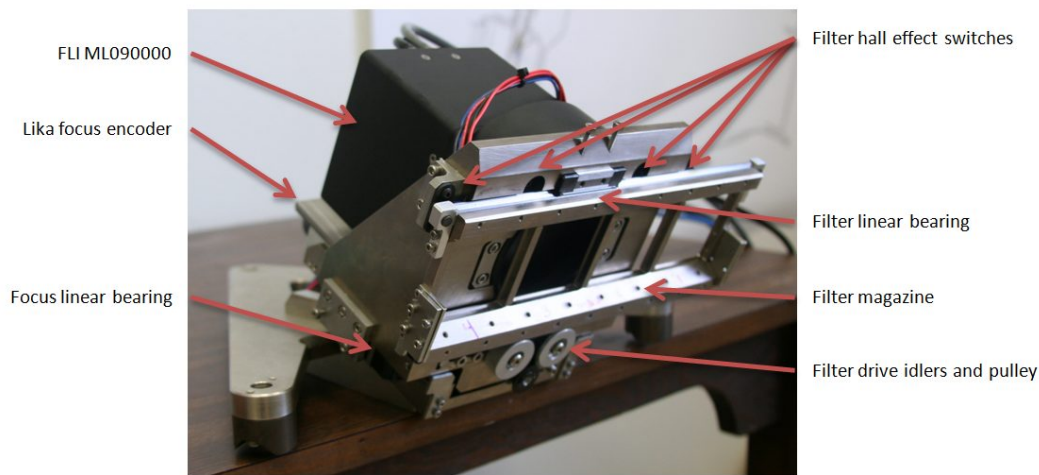


Figure 16. Photo of acquisition camera assembly.

2.6 Pupil Viewer and Calibration Wave Front Sensor

The pupil viewer and calibration wave front sensors are both optical metrology devices built around Allied Vision Technologies machine vision cameras. The pupil viewer has a collimating lens in custom housing mounted directly to a Manta G-033 camera with stock c-mount bayonet removed. The calibration wave front sensor has a custom housing for collimating optics and microlens array mounted to a Prosilica GC2450 camera. Both use gigabit Ethernet communications and are air-cooled. The two devices are mounted to a Festo SLF-10 pneumatic slide to share the optical feed from a pneumatically deployed fold mirror. The pupil viewer has a tip-tilt-focus adjustable mount and the calibration wave front sensor has a tip-tilt-focus adjustment and a rotational adjustment. A set of hall effect switches detect position of the pneumatic stage at ends of travel. Renderings of the instruments are shown in figure 17.

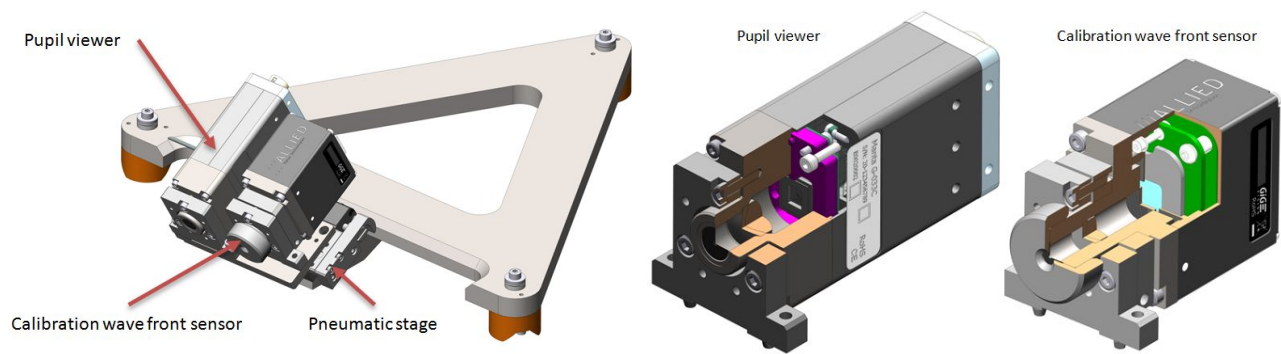


Figure 17. The complete pupil viewer/calibration wave front sensor assembly and sectional views of the two instruments

2.7 Fold Mirror Actuator

The fold mirror actuator deploys two mirrors to the center of the telescope field to feed light to the acquisition camera, pupil viewer and calibration wave front sensor. Each mirror is mounted to a steel arm with a tip-tilt-piston adjustment mechanism. The arm rides on a linear ball guide with factory set preload purchased from Misumi. Each arm is actuated by a Festo pneumatic cylinder. The cylinder is mounted inside the hollow annulus of the support arm. A set of hall effect switches at the ends of travel detect position of each mirror. A rendering of the assembly is shown in figure 18.

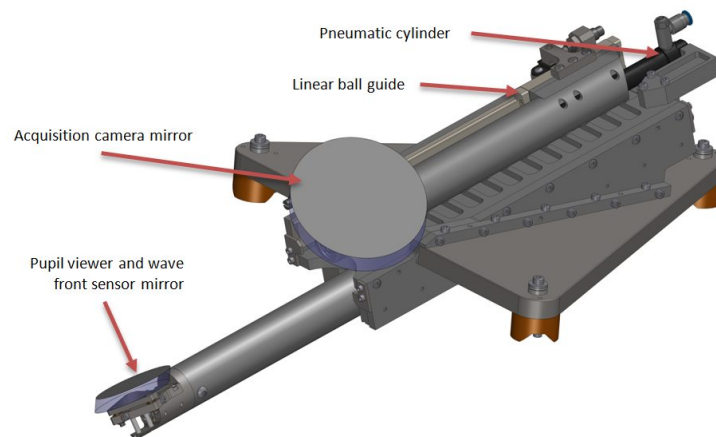


Figure 18. The fold mirror actuator for feeding the acquisition camera, pupil viewer, and calibration wave front sensor.

2.8 FPA Utilities Enclosure

The focal plane assembly utilities enclosure houses the control electronics for the acquisition and guiding instrumentation, the dithering mechanism, and shutter as well as the guider probe cameras. The enclosure also contains a pair of liquid-to-air heat exchangers with blowers to remove heat generated by the electronics. This air handling system includes glass fiber pre-filter and a HEPA filter for maintaining air quality inside the focal plane assembly. The heat exchangers were purchased from Lytron and are constructed of aluminum and specifically designed for the heat transfer properties of glycol. The blowers were purchased from Oriental Motor and powered by 24VDC. A glycol manifold is built into the enclosure to provide liquid cooling for 4 guide probes cameras and the acquisition camera. Connection between manifold and cameras are made with Swagelok QC4 quick disconnects with disconnect valves on both body and stem so that cameras can be removed and replaced without the possibility of spillage.

The enclosure is constructed primarily of carbon fiber laminated foam panels. The panels possess both high rigidity and thermal insulation. The material was purchased as custom cut panels from Allred Associates as 3-layer CFRP sheets laminated on Airex C70-40 foam. The panels were assembled with West Systems 105/206 epoxy. The air handling manifold and other aluminum hardware were also integrated into the enclosure using 3M brand 2216 epoxy.

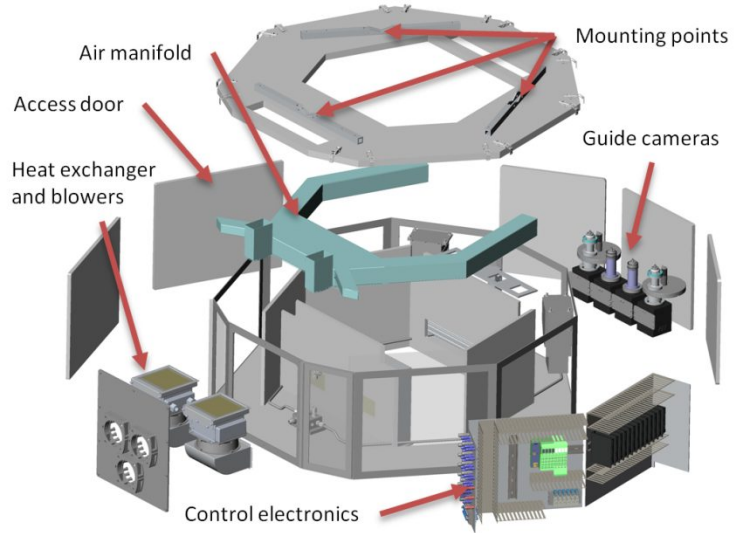


Figure 19, left shows the enclosure prior to painting, with dog for scale. Figure 20, right shows an exploded rendering of the enclosure and its internal hardware.

2.9 Weldments

The PFIP contains three mating steel weldments; the focal plane assembly frame, the acquisition and guiding frame, and the fixed instrument mounting frame. All three frames were fabricated by SMK Manufacturing from mild steel structural tubing and plate. The assemblies were all welded and post-machined to achieve a high level of accuracy of critical mounting surfaces. The focal plane assembly frame is the largest and supports all of the focal plane assembly components including the FPA utilities enclosure, the acquisition and guiding frame, the fixed instrument mount, the IFU strain relief, and enclosures. The focal plane assembly frame mounts to the Rho stage through a kinematic interface to allow removal and replacement with high repeatability of optical alignment with the Wide Field Corrector.

The acquisition and guiding frame supports the guide probe assembly, acquisition camera, calibration wave front sensor, pupil viewer, and fold mirror actuator. It mounts to the focal plane assembly frame through a kinematic interface to allow removal and replacement with high repeatability of optical alignment with the focal plane assembly.

The fixed instrument mounting frame is bolted to the focal plane assembly frame. It supports the shutter, the dithering mechanism, and the instrument feeds. The fixed instrument feed is a temporary feature, to be replaced by a two-position instrument changer after commissioning of the upgraded telescope. The three weldments are shown in an exploded CAD rendering in figure 20 and in a photo taken during integration and test in figure 21.

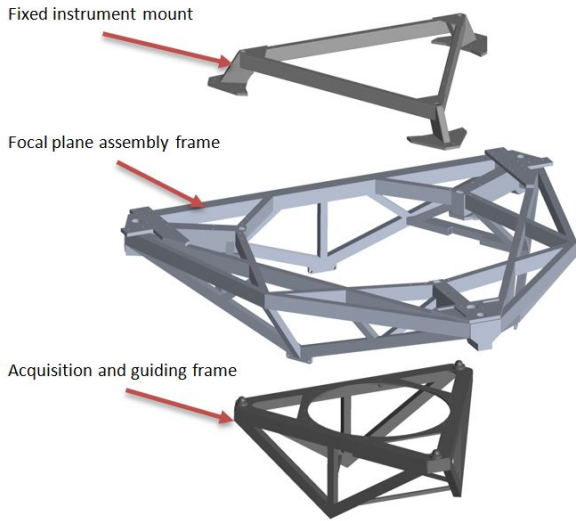


Figure 20, left shows an exploded rendering of the three weldments in the focal plane assembly. Figure 21, right shows a photo of the weldments during integration.

2.10 Lower Instrument Package

The Lower Instrument Package (LIP) is mounted to the input end of the wide field corrector and is a platform for the entrance window changer, tip-tilt camera, and facility calibration unit (FCU) output head. Figure 22 shows a rendering of the assembly.

The entrance window changer can select between three 184mm diameter windows. The three windows are mounted to a rotary stage which is designed to form a low-leak instrument air seal with the wide field corrector. Motion is guided with an angular contact bearing mounted at the center of the stage, with an adjustable preload that bears against a needle thrust bearing. The stage is actuated by a toothed belt stretched around the stage's perimeter and through a set of tensioning idlers and drive pulley. The drive pulley is coupled to a Maxon ECmax 30 motor through a worm-drive gear box. A set of three hall-effect sensors on the chassis detect window position and their outputs are wired to the Maxon motor controller. A homing mode is used to drive the stage position until the desired hall effect switch is triggered. Figure 23 shows an exploded view of the entrance window changer.

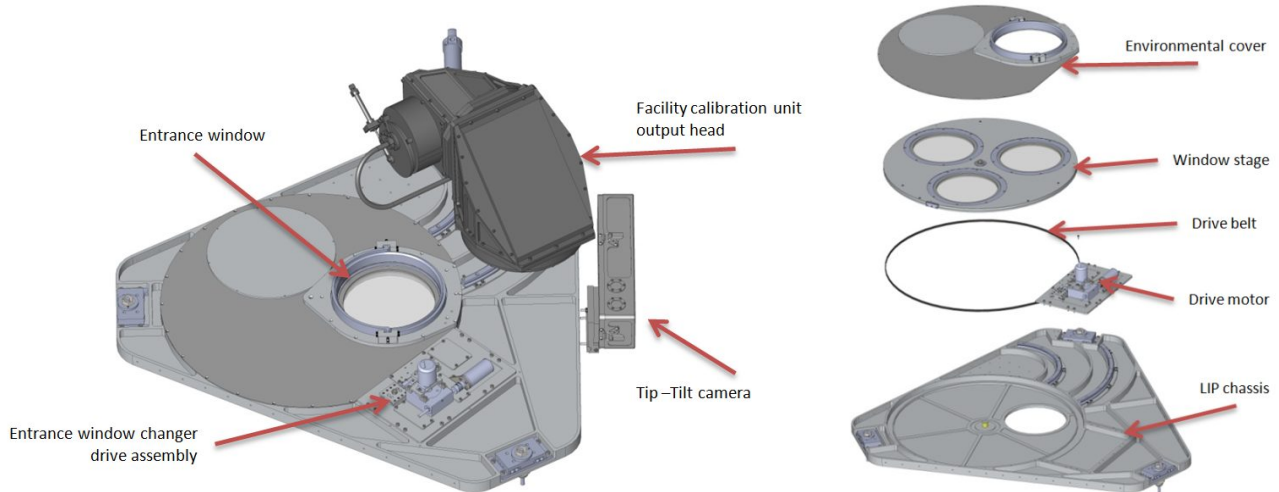


Figure 22, left shows a rendering of the lower instrument package. Figure 23, right shows an exploded view of the entrance window assembly

The tip-tilt camera, shown in figure 24, is used to detect the PFIP orientation with respect to the primary mirror. The device operates by directing a collimated 1550nm light source at the primary mirror. The reflected spot is incident to a 1550nm-to-visible converter lens assembly purchased from Edmund Optics. The converter lens is coupled to an Allied Vision Technologies Prosilica GC655 camera. Changes in the reflected spot position on the camera image indicate changes in the orientation of the device with respect to the primary mirror. The light source is an erbium-doped fiber amplifier purchased from Lightwaves2020 and collimated by an off-the-shelf fiber collimator with adjustable focus. Since the beam reflects from the spherical primary mirror, the collimator must be focused in-situ to obtain a suitable spot size once reflected onto the converter lens.

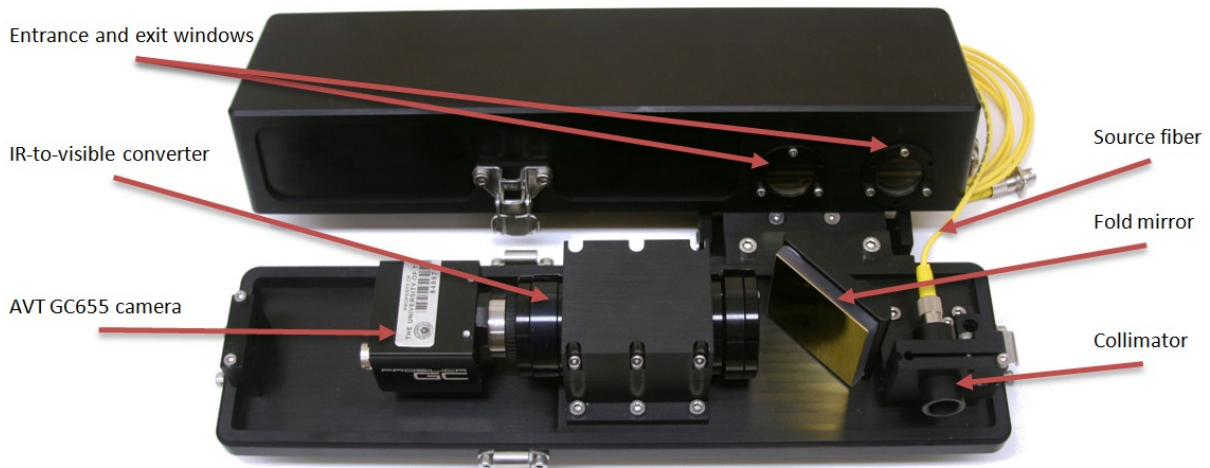


Figure 24. Photo of the tip-tilt camera.

2.11 Facility Calibration Unit

The facility calibration unit [6] provides a variety of reference light sources fed into the entrance of the wide field corrector (figures 25 and 26). An input assembly is located in a remote enclosure and contains the light sources and optics. Two liquid light guides transmit the light from the remote input assembly to a deployable output head mounted to the lower instrument package below the wide field corrector.

The input assembly can hold 10 penray, hollow cathode, or QTH lamps, separated into two banks of five lamps. A liquid light guide on each bank can be positioned to any of the five light sources. A third light guide is coupled to a LED-based light source. The three light guides transmit light from their respective sources to an optical mixing unit to combine the light from all three sources. The output of the optical mixing unit is fed into one of two liquid light guides which feed directly to the output head. A Festo SLF-10 pneumatic stage is used to select between the two light guides, with one guide optimized for blue wavelengths and the other optimized for red.

The source selector is a Festo SLG-12 pneumatic slide with integral ball guide and pneumatically deployed stops mounted mid-stroke. This off-the-shelf solution provides a way to position a source light guide over the multiple light sources with ball guide accuracy and the simplicity and reliability of a pneumatic actuator. Hall effect switches indicate the position of the source guide and the states of the deployable stops.

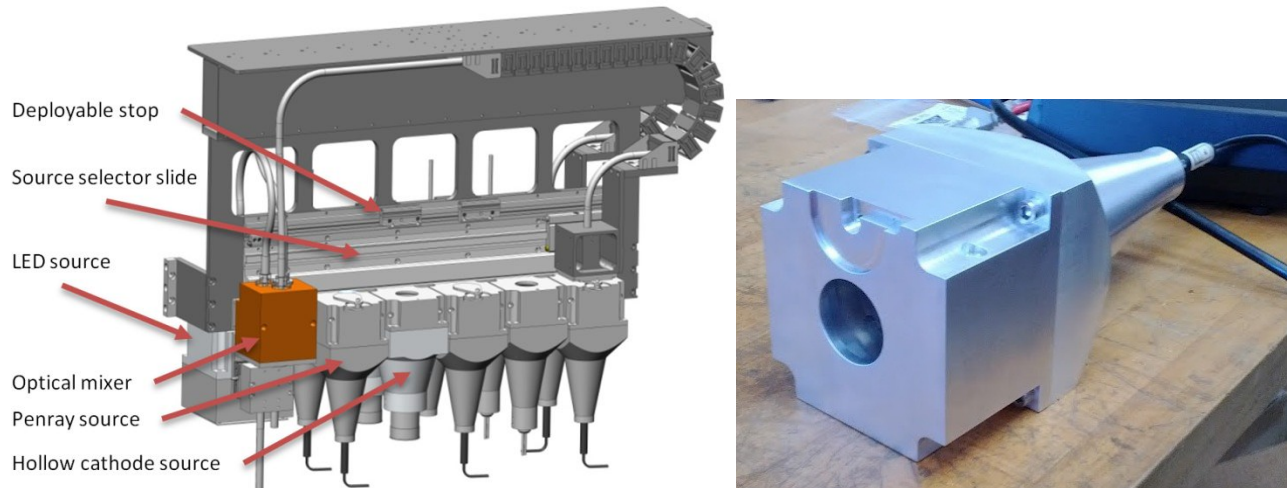


Figure 25, left shows a rendering of the FCU input assembly. Figure 26, right shows a photo of a penray source.

At the lower instrument package (figure 27), a pneumatic cylinder deploys and retracts the FCU output head at the entrance of the wide field corrector. When deployed, the output head forms a light-tight seal with the corrector to enable calibration during the day or with dome lights on. A set of optics in the output head shape the light to imitate the ray bundle arriving at the wide field corrector from the primary mirror. The output head also contains a two-position pneumatically actuated selector for controlling which of the two light guides are used. The blue-optimized light guide is positioned such that the entire telescope field is covered. The red-optimized light guide includes an additional optic and is positioned to cover only the telescopes field occupied by the high, medium, and low spectrograph feeds, but not the VIRUS feeds.

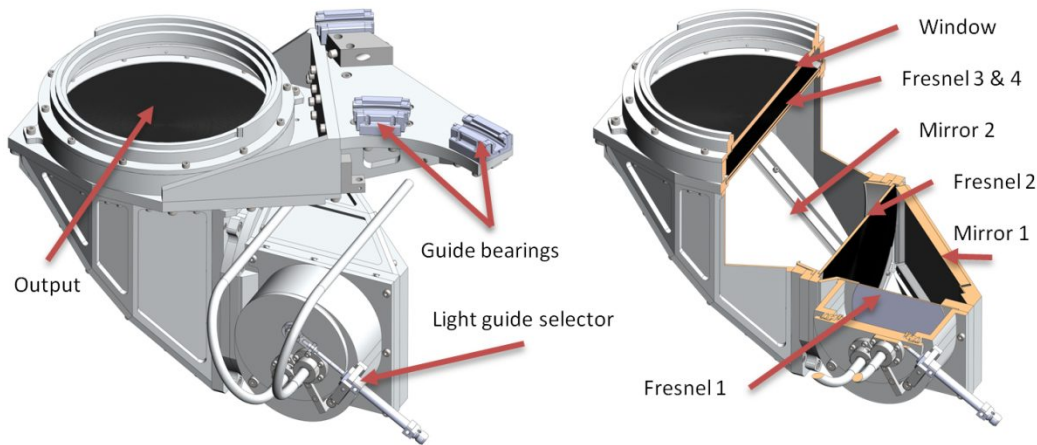


Figure 27. Rendering and sectional view of the facility calibration unit output head

3. NEXT STEPS

At this time, the PFIP subassemblies are undergoing continuing integration and test. Software for control of the PFIP is well underway, with a high-level architecture written as part of the telescope control system. Hardware level software is being written in LabView for the purposes of testing. Going forward, the high level software and hardware level software will need to be integrated.

Aligning the components of the focal plane assembly to each other and to the wide field corrector will also be developed further going forward. A set of alignment references and instrumentation has had initial design, and those will be refined and fabricated.

Electronics panels and cabling will also be built to their final arrangements. A set of Lemo 1B connectors has been chosen and cable lengths determined so final cable assemblies are ready to build.

ACKNOWLEDGEMENTS

HETDEX is run by the University of Texas at Austin McDonald Observatory and Department of Astronomy with participation from the Ludwig-Maximilians-Universität München, Max-Planck-Institut für Extraterrestrische-Physik (MPE), Leibniz-Institut für Astrophysik Potsdam (AIP), Texas A&M University, Pennsylvania State University, Institut für Astrophysik Göttingen, University of Oxford and Max-Planck-Institut für Astrophysik (MPA). In addition to Institutional support, HETDEX is funded by the National Science Foundation (grant AST-0926815), the State of Texas, the US Air Force (AFRL FA9451-04-2-0355), and generous support from private individuals and foundations.

REFERENCES

- [1] G.J. Hill, J.A. Booth, M.E. Cornell, J.M. Good, K. Gebhardt, H.J. Kriel, H. Lee, R. Leck, P.J. MacQueen, D.M. Perry, M.D. Rafal, T.H. Rafferty, C. Ramiller, R.D. Savage, C.A. Taylor III, B.L. Vattiat, L.W. Ramsey, J.H. Beno, T.A. Beets, J.D. Eguerra, M. Haueser, R.J. Hayes, J.T. Heisler, I.M. Soukup, J.J. Zierer, Jr., M.S. Worthington, N.T. Mollison, D.R. Wardell, G.A. Wedeking, "Current status of the Hobby-Eberly Telescope wide field upgrade," Proc. SPIE, **8444**-19 (2012)
- [2] H. Lee, G.J. Hill, M.E. Cornell, B.L. Vattiat, T.H. Rafferty, C.A. Taylor III, D.M. Perry, C. Ramiller, M. Hart, M.D. Rafal, R.D. Savage, "Metrology systems of Hobby-Eberly Telescope wide field upgrade," Proc. SPIE, **8444**-181 (2012)
- [3] J.H. Beno, C.E. Penney, R.J. Hayes, I.M. Soukup, "HETDEX tracker control system design and implementation," Proc. SPIE, **8444**-211 (2012)
- [4] J.J. Zierer, Jr., G.A. Wedeking, J.H. Beno, J.M. Good, "Design, testing, and installation of a high-precision hexapod for the Hobby-Eberly Telescope dark energy experiment (HETDEX)," Proc. SPIE, **8444**-176 (2012)
- [5] J. H. Burge, S. D. Benjamin, M. B. Dubin, S. M. Manuel, M. J. Novak, Chang Jin Oh, M. J. Valente, C. Zhao, J. A. Booth, J. M. Good, G. J. Hill, H. Lee, P. J. MacQueen, M. D. Rafal, R. D. Savage, M. P. Smith, B. L. Vattiat, "Development of a wide-field spherical aberration corrector for the Hobby Eberly Telescope", Proc. SPIE, **7733**-51 (2010)
- [6] H. Lee, G.J. Hill, B.L. Vattiat, M.P. Smith, M. Haueser, "Facility calibration unit of Hobby Eberly Telescope wide field upgrade," Proc. SPIE, **8444**-172 (2012)